Vibrational Stark Spectroscopy of NO Bound to Heme: Effects of Protein Electrostatic Fields on the NO Stretch Frequency

Eun Sun Park, Melissa R. Thomas, and Steven G. Boxer*

Contribution from the Department of Chemistry, Stanford University, Stanford, California 94305-5080

Received April 27, 2000. Revised Manuscript Received August 22, 2000

Abstract: The vibrational Stark effect measures the effect of an external electric field on the vibrational (IR) spectrum of a molecule. This technique gives quantitative information on the sensitivity of a vibrational peak position to an electric field. This calibration can be used to evaluate shifts in the vibrational frequency caused by changes in the local electric field in the organized electrostatic matrix of a protein, for example, by mutating amino acid residues near the vibration whose frequency is probed. We report vibrational Stark effect measurements for NO bound to several distal pocket mutants of myoglobin, (Val68Asp, Val68Asn, Val68Glu, and His64Val). These mutations were designed to perturb the electrostatic field near the NO bound to the heme iron. The magnitude of the change in dipole moment, $|\Delta\mu|$, for the vibration of NO bound to heme is found to be approximately 0.12 D/*f*, that is, the Stark tuning rate is $2.0/f$ cm^{-1}/(MV/cm) (where *f* is the local field correction) for a series of distal pocket mutants for which the vibrational frequency, $\bar{\nu}_{NO}$, varies by over 60 cm^{-1} and also for a picket fence model compound. Both $|\Delta\mu|$ and the dispersion of $\bar{\nu}_{NO}$ are similar to those reported for CO bound to the heme iron (Park, E. S.; Andrews, S. S.; Hu, R. B.; Boxer, S. G., *J. Phys. Chem. B* **1999**, *103*, 9813−9817). This correlation can be quantitatively explained if the dispersion in $\bar{\nu}_{NO}$ and $\bar{\nu}_{CO}$ is modeled as an electrochromic band shift due to the interaction of the change in dipole moment of the oscillator and the electric field of the protein. The slope of the correlation is given by the measured ratio $\Delta\mu_{NO}/\Delta\mu_{CO}$ obtained from the vibrational Stark effect data.

Introduction

Nitric oxide (NO) plays a central role in many biological processes. In nearly every case this involves the reaction of NO with heme proteins; the synthesis of NO is also catalyzed by heme proteins.[1] When bound to the heme iron, NO can be selectively detected in the infrared (IR),[2] and as with bound CO,[3] it is expected that variations in $\bar{\nu}_{NO}$ in different heme proteins and mutants of these proteins should be a sensitive probe of bonding and local electrostatics.

We recently reported a direct measurement of the magnitude and direction of the change in dipole moment, $\Delta\mu$, for the IR absorption of CO bound to wild-type (WT) myoglobin (Mb) and several Mb mutants by using vibrational Stark effect (VSE) spectroscopy.[4] This method provides quantitative information on the sensitivity of $\bar{\nu}_{CO}$ to an electric field and whether this sensitivity changes when the protein or matrix is perturbed. It is our contention that the variations in $\bar{\nu}_{CO}$ (and $\bar{\nu}_{NO}$, *vide infra*) in Mb distal pocket mutants are, in many cases, electrochromic band shifts due to the interaction between $\Delta\mu$ associated with the oscillator and the electric field due to the protein matrix F_{matrix}. Typically we measure the change in the matrix electric field, ΔF_{matrix}, for example when studying a series of mutants or protonation states compared with some standard state such as the wild-type protein at pH 7. In this case, the energy shift for a transition is $\Delta E = hc\Delta\bar{\nu} = -\Delta\mu\cdot\Delta F_{matrix}$, where $\Delta\bar{\nu}$ is the observed band shift in cm^{-1}.[5] In all Mb mutants studied to date, as well as for CO bound to a picket fence model compound and for CO bound to cytochrome *c*, $|\Delta\mu| \approx 0.14$ D/*f*, where *f* is the local field correction factor.[6] Furthermore, for wild-type MbCO, $\Delta\mu$ was found to be parallel to the transition moment, and the latter has been shown to be approximately perpendicular to the heme plane.[7−9] Therefore, the VSE measurements calibrate the CO oscillator as a probe that is sensitive to the magnitude and direction of the protein matrix electric field. Variations in $\bar{\nu}_{CO}$ can then be used to estimate differences in the field, and this provides a quantitative basis for correlations between calculated[10] and observed variations in $\bar{\nu}_{CO}$.

Despite the importance of the NO−heme interaction, the IR spectroscopy of NO has been studied much less than that of CO due to the difficulty of the experiments. The NO stretch vibration has a lower extinction coefficient than CO,[11] and, when NO is bound to the heme iron, $\bar{\nu}_{NO}$ overlaps with the intense

(1) Packer, L. Nitric Oxide Parts A and B. In *Methods in Enzymology*; Academic Press: San Diego, CA, 1996; Vols. 268 and 269.

(2) Miller, L. M.; Pedraza, A. J.; Chance, M. R. *Biochemistry* **1997**, *36*, 12199−12207.

(3) Li, T. S.; Quillin, M. L.; Phillips, G. N.; Olson, J. S. *Biochemistry* **1994**, *33*, 1433−1446.

(4) Park, E. S.; Andrews, S. S.; Hu, R. B.; Boxer, S. G. *J. Phys. Chem. B* **1999**, *103*, 9813−9817.

(5) In the previous paper (ref 4), we used F_{matrix} instead of ΔF_{matrix} in this expression. Because a matrix electric field is always present, the shift in the band measured upon varying the ionization state of a nearby residue or upon making a mutant is due to a change in the matrix field ΔF_{matrix}.

(6) The actual field felt by the chromophore in response to the externally applied electric field is usually called the internal field $F_{int} = f\cdot F_{ext}$. F_{int} is not to be confused with the electric field due to the surrounding protein, F_{matrix}. The local field correction *f* is in general a tensor quantity; it is treated here as a scalar, and the value of *f* should be somewhat greater than 1 (see ref 4 for a detailed discussion). Due to uncertainty in the value of *f*, we report the observed values of $|\Delta\mu|$ divided by *f*. See, e.g.: Böttcher, C. J. F. *Theory of Electric Polarization*; Elsevier: Amsterdam, 1973; Vol. 1.

(7) Lim, M.; Jackson, T. A.; Anfinrud, P. A. *Science* **1995**, *266*, 962−966.

(8) Ivanov, D.; Sage, J. T.; Keim, M.; Powell, J. R.; Asher, S. A.; Champion, P. M. *J. Am. Chem. Soc.* **1994**, *116*, 4139−4140.

(9) Sage, J. T.; Jee, W. *J. Mol. Biol.* **1997**, *274*, 21−26.

(10) Phillips, G. N.; Teodoro, M. L.; Li, T. S.; Smith, B.; Olson, J. S. *J. Phys. Chem. B* **1999**, *103*, 8817−8829.

10.1021/ja0014741 CCC: $19.00
Published on Web 11/21/2000

amide protein bands (amide I ≈ 1655 cm^{-1}, amide II ≈ 1555 cm^{-1}). Thus, photolysis difference FTIR spectroscopy at liquid He temperatures[2] or isotope difference FTIR spectroscopy[11] are needed to identify the NO stretch frequency. The difficulty is compounded for VSE measurements of NO bound to the protein because it is hard to get a good signal-to-noise Stark spectrum due to the intense absorption of amide bands. Furthermore, it is necessary to get the actual absorption amplitude and line shape of the NO peak for a quantitative analysis of the Stark analysis.[12]

In the following we report the first VSE measurements for NO bound to a picket fence porphyrin and several distal pocket mutants of Mb which were designed to perturb the electrostatic field near the heme as probed by iron redox potential shifts,[13] pK_a and spectral shifts,[14] and IR band shifts.[4,15] We also report $\bar{\nu}_{NO}$ for the same distal pocket mutants of Mb and compare the results with those obtained earlier for $\bar{\nu}_{CO}$.[15,16] We find that the dispersion for $\bar{\nu}_{NO}$ correlates with that for $\bar{\nu}_{CO}$ in the same mutants. This dispersion in both $\bar{\nu}_{NO}$ and $\bar{\nu}_{CO}$ can be consistently modeled as electrochromic band shifts, and the variations are quantitatively explained by the measured ratio $\Delta\mu_{NO}/\Delta\mu_{CO}$ obtained from the VSE data.

Materials and Methods

Sample Preparation. Wild-type human Mb[17] and the V68D, V68N, and V68E variants were expressed and purified from *Escherichia coli* as described elsewhere.[14] All proteins also contain the surface mutation C110A to improve the yield upon purification; this mutation does not significantly perturb the structure and ligand binding properties. Sperm whale Mb mutant, H64V, was also prepared and purified as described previously.[18] Protein solutions were concentrated to ~4 mM in 50/50 glycerol/buffer (100 mM phosphate buffer, pH 7). Samples were purged with N_2 gas to remove oxygen and reduced with ~3 equiv of 1 M aqueous sodium dithionite. The solutions were then immediately placed under NO (^{14}NO: natural abundance, Matheson; ^{15}NO: 99% isotopic purity, Isotec). Formation of the MbNO complexes was confirmed by monitoring the UV/vis absorption spectrum.

Iron(III) *m*-tetrakis (α,α,α,α,-*o*-pivalaminophenyl) porphyrin (picket fence porphyrin) bromide salt was purchased from Mid-Century Chemicals and used without further purification. Anhydrous 2-methyl tetrahydrofuran (2-MeTHF) and imidazole (Im) were purchased from Aldrich. 2-MeTHF was purged with N_2 gas to remove oxygen before use. The picket fence porphyrin (PF) and Im were dissolved in 2-MeTHF and the solution was purged further with N_2 gas. The sample was reduced with ~3 equiv of 1 M aqueous sodium dithionite solution and immediately placed under NO. The final concentration varied from sample to sample due to some evaporation of the solvent during purging but was approximately 8 mM porphyrin and 100 mM Im. Formation of the six-coordinate PF(Im)(NO) porphyrin complex was confirmed by the UV/vis absorption spectrum.

Photolysis Difference FTIR spectroscopy. Photolysis difference FTIR spectra were obtained on a Bruker IFS 66V/S FTIR spectrometer (2 cm^{-1} resolution) using an MCT detector. The samples were loaded into an IR cell made with CaF_2 windows and ~25 μm Teflon spacers, attached to the coldfinger of a continuous-flow liquid helium cryostat and then cooled to 5 K. Spectra were taken at 5 K before and after photolysis of bound NO using a 300 W halogen lamp. An IR filter was placed between the lamp and the sample to prevent sample heating. The photolysis difference spectrum [Δ*A*(photolyzed minus unphotolyzed)] gives the spectrum predominantly of the NO ligand bound to Mb since a substantial fraction of the sample with the NO photolyzed off the heme can be trapped at this temperature. The specific assignment of absorption changes associated with NO was achieved by isotope substitution.

Isotope Difference Spectroscopy. The absorption spectrum of a sample with ^{14}NO bound (WT and V68E) or ^{15}NO bound (H64V and V68D) was taken on the same FTIR spectrometer with 2 cm^{-1} resolution at 74 K right after taking its Stark spectrum. This absorption spectrum of ^{14}NO or ^{15}NO bound Mb was later subtracted from that of ^{15}NO or ^{14}NO bound Mb, respectively, at approximately the same concentration, giving the isotope difference spectrum (^{14}NO minus ^{15}NO or ^{15}NO minus ^{14}NO, respectively). The isotope difference spectra were used for the later Stark analysis. The isotope difference spectra typically had sloping baselines due to imperfections in the subtraction process, and this baseline was removed to facilitate the Stark analysis. The NO absorption peak in the isotope difference spectrum was fitted with a sum of Lorentzian and Gaussian line shapes; the analytical second derivative of this best fit[19] was used in fitting the Stark data (see below). When the NO Stark peak overlaps with a broad amide Stark peak and thus has a sloping baseline, a straight line was also added in fitting the Stark data.

Vibrational Stark Spectroscopy. The absorption and VSE spectra were taken on the same FTIR spectrometer with 0.5 cm^{-1} resolution. The samples were loaded into a homemade IR cell made from a pair of Ni-coated (~50 Å thick Ni) CaF_2 windows separated by ~30 μm Teflon spacers. The Ni coating acts as a semitransparent electrode for application of an electric field across the sample. The cell containing the samples was immersed in a custom-built liquid N_2 immersion cryostat that operates at approximately 74 K.[20] To get a good signal-to-noise ratio, the electric field was typically applied to the sample parallel to the IR beam so that unpolarized light can be used. A single scan was obtained with the field off, then a scan with the field on (typically about +2.5 kV), then another scan with the field off, and finally a scan with the same magnitude of the field on, but in the opposite direction. This cycle was repeated at least 512 times for each Stark spectrum that is the average of the field-on scans minus the average of the field-off scans. At least three such VSE measurements were performed for each sample with different electric fields (1.5−2.75 kV, corresponding to an applied field of 0.5−1 MV/cm). Further experimental details on the setup, including a general schematic for Stark experiments, are reported elsewhere.[12,21] For the polarization measurements, a horizontally transmitting IR polarizer was inserted between the detector and the cryostat, and the sample cell was rotated about the vertical axis to change the angle χ between the direction of the applied electric field and the electric vector of the polarized light.

Analysis of VSE Data. For an immobilized, isotropic sample, the Stark spectrum can be described as a sum of derivatives of the absorption spectrum:[12]

$$\Delta A(\bar{\nu}) = (F_{ext}\cdot f)^2\left\{A_\chi A(\bar{\nu}) + \frac{B_\chi}{15hc}\bar{\nu}\frac{d}{d\bar{\nu}}\left(\frac{A(\bar{\nu})}{\bar{\nu}}\right) + \frac{C_\chi}{30h^2c^2}\bar{\nu}\frac{d^2}{d\bar{\nu}^2}\left(\frac{A(\bar{\nu})}{\bar{\nu}}\right)\right\} \quad (1)$$

where F_{ext} is the external applied field, f is the local field correction,[6] h is Planck's constant, and c is the speed of light. The coefficients A_χ, B_χ, and C_χ are associated with molecular properties of the system. A_χ is related to the change in the transition moment upon application of

(11) Zhao, X. J.; Sampath, V.; Caughey, W. S. *Biochem. Biophys. Res. Comm.* **1994**, *204*, 537−543.
(12) Bublitz, G. U.; Boxer, S. G. *Annu. Rev. Phys. Chem.* **1997**, *48*, 213−242.
(13) Varadarajan, R.; Zewert, T. E.; Gray, H. B.; Boxer, S. G. *Science* **1989**, *243*, 69−72.
(14) Varadarajan, R.; Lambright, D. G.; Boxer, S. G. *Biochemistry* **1989**, *28*, 3771−3781.
(15) Decatur, S. M.; Boxer, S. G. *Biochem. Biophys. Res. Commun.* **1995**, *212*, 159−164.
(16) Balasubramanian, S.; Lambright, D. G.; Boxer, S. G. *Proc. Natl. Acad. Sci. U.S.A.* **1993**, *90*, 4718−4722.
(17) Varadarajan, R.; Szabo, A.; Boxer, S. G. *Proc. Natl. Acad. Sci. U.S.A.* **1985**, *82*, 5681−5684.
(18) Springer, B. A.; Sligar, S. G. *Proc. Natl. Acad. Sci. U.S.A.* **1987**, *84*, 8961−8965.

(19) There is no physical meaning associated with the line shape functions; these are simply used to obtain numerical derivatives of the absorption spectrum used in fitting the Stark data (eq 1). The contributions from the zeroth derivative and the first derivative are fairly small. Thus, we ignored these contributions to facilitate fitting when the signal-to-noise of the spectrum was not great. See the text for details.

(20) Andrews, S. S.; Boxer, S. G. *Rev. Sci. Instrum.*, **2000**, *71*, 3567−3569.
(21) Andrews, S. S.; Boxer, S. G. *J. Phys. Chem.* **2000**, in press.

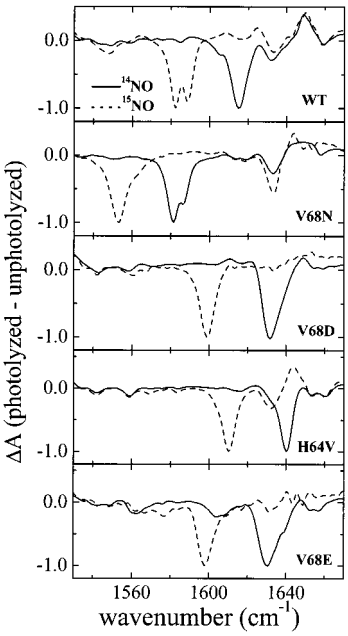

Figure 1. Photolysis difference absorption spectra (photolyzed minus unphotolyzed) of MbNO at 5 K in 50% glycerol/phosphate buffer at pH = 7 for the indicated Mb distal pocket variants. The spectra are normalized for unit absorbance difference at the maximum of the difference spectrum (the actual difference was typically $\Delta A \approx 0.01$). The solid lines are difference spectra for Mb^{14}NO; the dashed lines are for Mb^{15}NO.

an applied field, B_χ is associated with the change in polarizability, $\Delta\alpha$, between the ground and excited states and the transition polarizability, and C_χ, the coefficient of the second derivative contribution to the Stark line shape, is given by:

$$C_\chi = |\Delta\mu|^2[5 + (3\cos^2\chi - 1)(3\cos^2\zeta - 1)] \qquad (2)$$

C_χ depends only on $\Delta\mu$ and ζ, the molecule-fixed angle between $\Delta\mu$ and the transition moment direction. ζ is determined from the ratio of the Stark spectra taken at different experimental angles χ between the direction of light polarization and the applied field direction. The coefficients in eq 1 are obtained by fitting the numerical derivatives of the absorption spectrum to the Stark spectrum.[12]

Results

IR Spectra of the NO Stretch. The photolysis difference IR spectra of NO in wild-type, V68N, V68D, V68E, and H64V MbNO are shown in Figure 1. The spectra were taken for both ^{14}NO and ^{15}NO to assign the bands associated with $\bar{\nu}_{NO}$. All NO bands show ~30 cm^{-1} isotope shifts as predicted from a reduced mass calculation for ^{14}NO compared with ^{15}NO, assuming that NO is an isolated oscillator.[2] Additional small bands that do not show the isotope effect are also seen in the difference spectra. These are due to small changes in the protein structure or electrochromic band shifts of heme or protein bands that occur upon photolysis. The NO band splits into two peaks when it absorbs near 1585 cm^{-1}, for example in the WT ^{15}NO and V68N ^{14}NO spectra. This is consistent with the previous observation that a Fermi resonance occurs between the NO stretch frequency and a C_β−C_β stretch (ν_2) in the porphyrin that occurs at 1583 cm^{-1};[22] the splitting does not appear in the difference spectrum unless $\bar{\nu}_{NO}$ is close to this value. It is also found that little ligand rebinding occurs when NO is photolyzed at 5 K except in V68E. In the case of V68E, the NO peak intensity in the steady-state photolysis difference spectrum is about 4 times smaller than the others even though the concentration of the sample is approximately the same. The peak in the difference spectrum becomes significantly smaller if scanned several minutes after stopping irradiation. Both results are consistent with significant NO recombination in V68E, which is not observed in wild-type and the other mutants.

(22) Tomita, T.; Hirota, S.; Ogura, T.; Olson, J. S.; Kitagawa, T. *J. Phys. Chem. B* **1999**, *103*, 7044−7054.

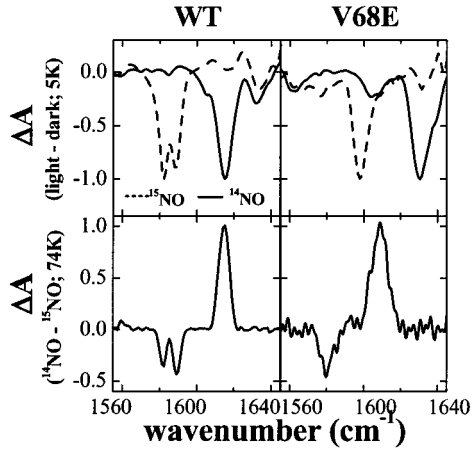

Figure 2. Photolysis difference (photolyzed minus unphotolyzed) and isotope difference (^{14}NO minus ^{15}NO) spectra of NO bound WT (left) and V68E (right) Mb are shown in top panels and bottom panels, respectively. The solid lines and dashed lines in the upper panels are for Mb^{14}NO and Mb^{15}NO, respectively. Samples were in 50% glycerol/phosphate buffer at pH = 7. Photolysis difference spectra were taken at 5 K, and isotope difference spectra were taken at 74 K.

When substantial rebinding occurs, photolysis difference spectroscopy may not give the actual ground-state absorption spectrum for NO bound to Mb. All Stark measurements were performed at 74 K where rebinding of the photolyzed NO occurs very rapidly. Thus, photolysis difference spectroscopy cannot be performed at 74 K to obtain the absorption spectrum of NO bound to Mb which is required to obtain the derivatives that are needed for the Stark analysis (eq 1), and this led us to obtain isotope difference spectra at 74 K. The isotope difference spectra of NO bound to wild type and V68E are compared with the photolysis difference spectra in Figure 2. The upper panels show the photolysis difference spectra, and the bottom panels show the isotope difference spectra. Typically, isotope difference spectra show residual amide bands, and the peak areas of ^{14}NO and ^{15}NO are different because it is difficult to exactly match the ^{14}NO and ^{15}NO sample concentrations. It is seen that the spectra of NO bound to wild-type are very similar and have $\bar{\nu}_{NO}$ at the same wavenumber whether obtained by photolysis at 5 K or isotope difference at 74 K (left panels Figure 2).[23] This is also true for other MbNO complexes except V68E (isotope difference spectra for V68D and H64V are shown in Figure 8 along with the Stark spectra and are very similar to the photolysis difference spectra in Figure 1; V68N is not shown). For NO bound to V68E, it is found that the major peak in the photolysis difference spectrum does not match the NO peak observed in the isotope difference spectrum. Note that isotope shifts observed in both types of difference spectra are consistent with a reduced mass calculation for ^{14}NO compared with ^{15}NO.[2] Comparison of the photolysis and isotope difference spectra suggests that the NO band from the major substate has a much lower rebinding barrier than that from the minor

(23) It is unlikely that there is any temperature dependence of the peak position in the absorption spectra between 5 and 74 K since samples were frozen rapidly in both cases so that they retain the population ratio at room temperature.

Table 1: Infrared Spectral Peak Positions of $\bar{\nu}_{NO}$ and $\bar{\nu}_{co}$ in Myoglobin Variants

protein[b]	$\bar{\nu}_{14NO}$ (cm^{-1})	$\bar{\nu}_{15NO}$ (cm^{-1})	$\bar{\nu}_{CO}$ (cm^{-1})[a]
wild-type	1615	1582.5, 1588.5[c]	1945
V68N	1581, 1586[c]	1553	1925[d]
V68D	1631.5	1600	1973[d]
V68E[e]	1630 (photolysis) 1609 (isotope)	1597.5 (photolysis) 1579.5 (isotope)	1937[d]
H64V	1640	1610	1970

[a] Data are taken from ref 15. [b] WT, V68N, V68D, and V68E are human Mb. H64V is SW Mb. [c] The peak is split into two peaks near 1585 cm^{-1} due to a Fermi resonance; see text. [d] Only the major peak positions are given.[40] [e] Photolysis difference spectroscopy and isotope difference spectroscopy give a different peak position for NO bound to V68E; see text and Figure 2.

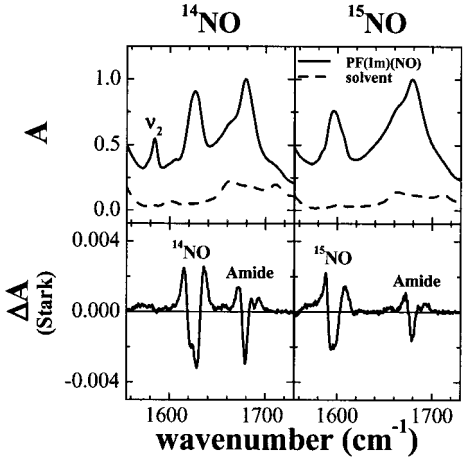

Figure 3. Absorption spectra (top panels, solid lines) and vibrational Stark spectra (bottom panel) for PF(Im)(NO) in 2MeTHF at 74 K. Left panels are for ^{14}NO bound and right panels are for ^{15}NO bound samples. The dashed lines in the top panels are the absorption spectra of 2MeTHF. The Stark spectra are scaled to 1 MV/cm applied electric field and are normalized for unit absorbance for a peak maximum. The actual maximum absorbance is ~0.3.

substate. In the case of the photolysis difference experiment, the peak intensity reflects both the population of the substate and the rebinding barrier. Thus, because the major substate has a lower rebinding barrier than that of the minor substate, the minor substate is prominent in the photolysis difference spectrum. When significant rebinding occurs even at 5 K, as in the case of V68E-NO, photolysis difference spectroscopy may give misleading information on the true absorption spectrum, and isotope difference spectroscopy should be performed to identify the NO stretch frequency of the predominant component.[24] The NO stretch frequencies in Mb variants are summarized along with the CO stretch frequencies in Table 1.

Vibrational Stark Spectroscopy. Figure 3 shows the absorption and VSE spectra of the PF(Im)(NO) complex. It is observed that isotope substitution shifts the peak at 1626 cm^{-1} in the spectrum of the PF(Im)(^{14}NO) complex to 1596 cm^{-1} and does not shift other peaks. This 30 cm^{-1} shift agrees with the expected isotope shift based on a reduced mass calculation, confirming that $\bar{\nu}_{NO}$ = 1626 cm^{-1} for PF(Im)(^{14}NO). The peak at 1584 cm^{-1} is likely a $C_\beta-C_\beta$ stretch (ν_2) in the porphyrin which causes a Fermi resonance with the NO band in some Mb mutants. The peak at 1679 cm^{-1} is assigned to the amide groups

(24) Vibrational Stark spectroscopy can also be a good way to identify the NO stretch peaks in the ground state, and this is seen for V68E-NO in Figure 7. Since the Stark spectrum has the second derivative line shape of the absorption, the overlap with the broad amide bands can be reduced. In addition, $|\Delta\mu|$ for NO bound to Mb is much larger than for amide bands.

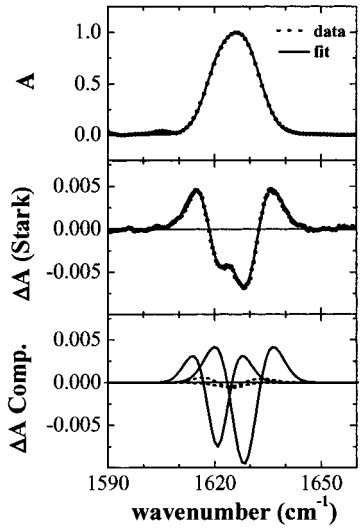

Figure 4. Absorption spectra (top panel, dotted curve), vibrational Stark spectra (middle panel, dotted curve), and (bottom panel) decomposition of the Stark spectrum into contributions from the second derivative (solid lines) and first derivative (dashed lines) of the absorption for PF(Im)(^{14}NO) in 2MeTHF at 74 K. The solid lines in the absorption and Stark panels are the best fits of absorption and Stark data, respectively.

in the PF porphyrin. The Stark spectrum of PF(Im)(NO) complex is dominated by the Stark effects of NO and the amide groups;[25] the Stark effect of the porphyrin ν_2 band is too small to measure.

The absorption and VSE spectra of ^{14}NO bound to PF(Im)-(^{14}NO) are shown on an expanded scale in the top panel and the middle panels, respectively, of Figure 4. The NO band consists of two peaks absorbing at 1621 and 1628 cm^{-1}; this is more clearly seen in the Stark spectrum, which is nearly identical to the second derivative of the absorption spectrum. This means that there is a very small contribution from the first derivative and that $|\Delta\mu|$ for both absorption features is essentially identical. Inspection of the VSE spectrum of the ^{15}NO complex shows that it also has two peaks, although it is difficult to see this in the absorption spectrum because of its overlap with the porphyrin ν_2 band and a solvent peak at 1601 cm^{-1}. The origin of these two peaks is not known. The best fit to the absorption and Stark spectra are overlaid on the data, and the decomposition of the Stark spectra into a sum of the first and second derivatives of the absorption is shown in the bottom panel (no contribution from the zeroth derivative was measured). This confirms that the vibrational Stark effect is completely dominated by the second derivative contribution due to $\Delta\mu$. Figure 5 shows the dependence of C_χ on $(3\cos^2\chi - 1)$ for the peaks at 1621 and 1628 cm^{-1}. Both fit well to a straight line and show that ζ is close to 0° for both peaks. Using this value, $|\Delta\mu|$ was calculated using eq 2, giving 0.104 D/f and 0.110 D/f for the peaks at 1621 and 1628 cm^{-1}, respectively.

Figure 6 shows the IR absorption in the 1500−1750 cm^{-1} region of the WT Mb^{14}NO complex and the VSE spectra of the ^{14}NO and ^{15}NO complexes (the IR absorption spectrum of WT Mb^{15}NO is very similar to that of WT Mb^{14}NO). The absorption is dominated by the intense amide I (1655 cm^{-1}) and amide II (1555 cm^{-1}) bands. As seen in photolysis and isotope difference spectra (Figure 2, left panels), ^{14}NO bound to WT Mb has an absorption at 1615 cm^{-1}; however, its

(25) The $|\Delta\mu|$ for the amide I band obtained from the Stark analysis is 0.08 D/f in both PF model compound and Mb and that for the amide II band is 0.07 D/f in Mb.

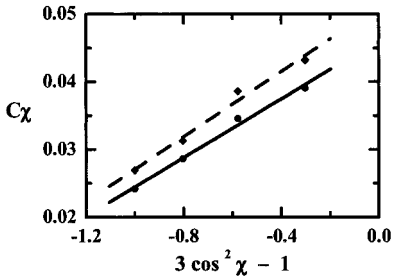

Figure 5. The second derivative contribution C_χ to the Stark spectrum vs $(3\cos^2\chi - 1)$, where χ is the experimental angle between the applied field direction and the electric vector of the polarized light used to probe the VSE (eq 2). The data are for PF(Im)(^{14}NO) in 2MeTHF. The circles represent the peak at 1621 cm^{-1}, and the diamonds are for the peak at 1628 cm^{-1}. The solid line and the dashed line are the linear fits for the circles and the diamonds, respectively, using eq 2 giving $\zeta = 0°$ and $|\Delta\mu| = 0.104$ D/*f* and 0.110 D/*f*, respectively.

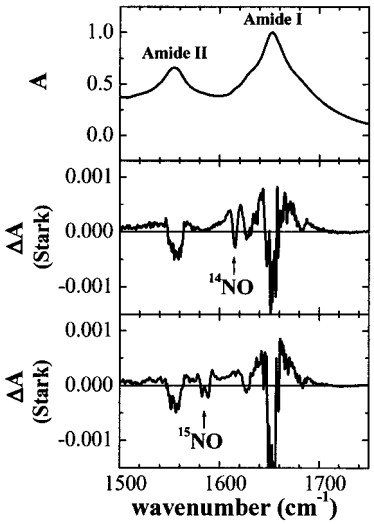

Figure 6. (Top panel) IR absorption spectrum in the 1500−1750 cm^{-1} region for ^{14}NO bound to WT. The spectrum is completely dominated by the amide I and amide II bands. The vibrational Stark spectra for ^{14}NO bound and ^{15}NO bound WT Mb in pH 7, 50% glycerol/phosphate buffer at 74 K, are shown in the middle and lower panels, respectively. The Stark spectra are scaled to 1 MV/cm applied electric field (eq 1) and are normalized for unit absorbance for a peak maximum. The actual maximum absorbance for amide I is ∼2.5 which accounts for the high noise on the Stark spectrum for this peak. Note that the peak due to bound ^{14}NO or ^{15}NO can be readily detected in the Stark spectrum, although it cannot be seen in the absorption spectrum due to the large background from the protein.

absorption band is buried under the huge amide bands. Nonetheless, there is a clear feature in the VSE spectrum of the WT Mb^{14}NO complex at 1615 cm^{-1}. We confirmed that the peak in the Stark spectrum at 1615 cm^{-1} is from ^{14}NO bound to WT Mb by obtaining the Stark spectrum for the Mb^{15}NO complex (Figure 6, bottom panel); the peak at 1615 cm^{-1} is shifted to ∼1585 cm^{-1} by the isotope substitution. The peak in the Stark spectrum at ∼1585 cm^{-1} is split by a Fermi resonance, consistent with what was observed in the photolysis difference and isotope difference spectra.[26] Since the Stark spectrum is the second derivative of the absorption line shape and the Stark

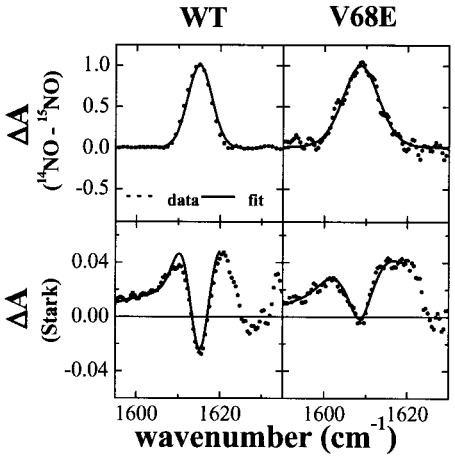

Figure 7. Isotope difference (^{14}NO minus ^{15}NO) absorption spectrum (top left panel, dotted curve) and vibrational Stark spectrum (bottom left panel, dotted curve) for NO bound to WT Mb and isotope difference (^{14}NO minus ^{15}NO) absorption spectrum (top right panel, dotted curve) and vibrational Stark spectrum (bottom right panel, dotted curve) for NO bound to V68E Mb in pH = 7, 50% glycerol/phosphate buffer. The spectra were taken at 74 K. The solid lines in the absorption and Stark panels are the best fits for NO bound to heme. The Stark spectra are scaled to 1 MV/cm applied electric field and are normalized for unit absorbance of NO vibration in the isotope difference spectra to facilitate comparison. The actual absorbances are approximately 0.01∼0.02.

effect for NO bound to Mb is large (see below), the NO peak can be observed in the Stark spectrum even though it is buried in the absorption spectrum. The Stark effects for the amide I and amide II bands are also seen in both Stark spectra.[25] The VSE for the amide bands is very noisy because of the low transmission in these concentrated samples that were optimized for the NO band. Note that the subbands of amide I shown as shoulders in the absorption spectrum are seen in the Stark spectrum at ∼1630 and ∼1680 cm^{-1}. These absorption subbands have been observed for Mb in the literature and have been suggested to arise from turns within the Mb, while the major band at ∼1655 cm^{-1} arises from a helix secondary structure.[27,28] Vibrational Stark spectra for amide bands in simple molecules, peptides, and proteins will be reported in a subsequent contribution.

To analyze the Stark spectrum quantitatively, we need the absorption spectrum taken under identical conditions. As discussed above, the only way to get the absorption spectrum for NO bound to the protein at 74 K is by isotope difference spectroscopy, although it is very difficult to take the difference between two separate samples with strongly overlapping absorption bands and obtain a flat baseline. The isotope difference absorption (^{14}NO minus ^{15}NO) and Stark spectra of ^{14}NO bound to WT and V68E are shown in Figure 7. ^{14}NO in V68D and H64V MbNO complexes has an absorption very close to the amide I band; therefore, the VSE spectra were obtained by using ^{15}NO instead of ^{14}NO to facilitate the analysis and to improve the signal-to-noise.[29] In these cases, the relevant isotope difference absorption spectra are ^{15}NO minus ^{14}NO; these spectra and the Stark spectra of ^{15}NO bound to V68D and H64V Mb are shown in Figure 8. The VSE experiment was not attempted for V68N since the ^{14}NO peak is split by Fermi

(26) The analysis of the Stark spectrum becomes more complex when a Fermi resonance occurs. For ^{15}NO in WT MbNO, the Stark line shape is quite different from the second derivative of the absorption, and the Stark effect seems much weaker than when there is no Fermi resonance. Apparently not only intensity borrowing occurs, but the value of $|\Delta\mu|$ is affected by a Fermi resonance with the porphyrin $\bar{\nu}_2$ band. This interesting phenomenon is not fully understood.

(27) Nabet, A.; Pezolet, M. *Appl. Spectrosc.* **1997**, *51*, 466−469.
(28) Jackson, M.; Mantsch, H. H. *Crit. Rev. Biochem. Mol. Biol.* **1995**, *30*, 95−120.

(29) It is observed that $|\Delta\mu|$ for ^{14}NO is the same as that for ^{15}NO within experimental error when there is no Fermi resonance involved.

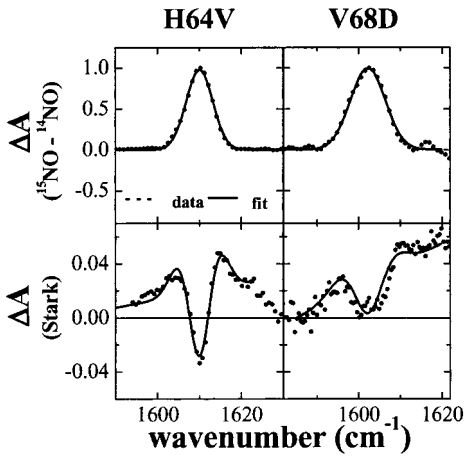

Figure 8. Isotope difference (^{15}NO minus ^{14}NO) absorption spectrum (top left panel, dotted curve) and vibrational Stark spectrum (bottom left panel, dotted curve) for NO bound to H64V Mb and isotope difference (^{15}NO minus ^{14}NO) absorption spectrum (top right panel, dotted curve) and vibrational Stark spectrum (bottom right panel, dotted curve) for NO bound to V68D Mb in pH = 7, 50% glycerol/phosphate buffer. The spectra were taken at 74 K. The solid lines in the absorption and Stark panels are the best fits for NO bound to heme. The Stark spectra are scaled to 1 MV/cm applied electric field and are normalized for unit absorbance of NO vibration in the isotope difference spectra to facilitate comparison.

resonance and the ^{15}NO peak is very close to the amide II band.[26] As seen in the figures, the NO Stark peak is on top of another broad Stark peak, and a straight line was used to fit the baseline of the NO Stark peak. The fits to the absorption and Stark spectra are overlaid on the data. The values of $|\Delta\mu|$ for NO obtained from the quantitative analysis assuming that $\zeta = 0°$ (see discussion) are 0.12−0.13 D/f in all MbNO complexes investigated, that is, they are the same within experimental error and also close to that measured in PF porphyrin.

Discussion

The spectra in Figures 6−8 demonstrate that VSE data can be obtained for NO bound to a protein even though the peak itself cannot be detected directly in the IR spectrum (Figure 6). This is because $|\Delta\mu|$ is *very* large when NO is bound to the heme iron as compared with other features in the IR spectrum. The Stark effect scales as $|\Delta\mu|^2$ and is most prominent for narrow features that have large second derivatives (eqs 1 and 2). The greatest limitation is our ability to obtain the absorption spectrum to characterize the derivatives, but even when the signal-to-noise ratio is poor, it is possible to extract quantitative information on $|\Delta\mu|$. The results show that $|\Delta\mu|$ is the same within the error of the measurement for a series of distal pocket mutants, despite the large variation in $\bar{\nu}_{NO}$ for this series. Furthermore, $|\Delta\mu|$ for NO bound to the picket fence model compound is essentially the same as in the proteins. We have not obtained the VSE spectrum for free NO, but *ab initio* calculations[30] suggest that $|\Delta\mu|$ is much smaller than what is observed when NO is bound to heme. As for CO,[4] the Stark data cannot distinguish whether the large value of $|\Delta\mu|$ when NO is bound to heme is due to enhanced bond anharmonicity or contributions from charge-separated resonance structures that are not accessible to the isolated diatomic.[31] Irrespective of the molecular origin of the effect, the observed value of $|\Delta\mu|$ can be translated into a Stark tuning rate of 2.0/f cm^{-1}/(MV/cm). The Stark tuning rate expresses explicitly the sensitivity of $\bar{\nu}_{NO}$ to external or matrix (protein) electric fields, that is, $\bar{\nu}_{NO}$ shifts by approximately 2 cm^{-1} when the projection of the matrix electric field along the direction of $\Delta\mu$ changes by 1 MV/cm.

The electrochromic band shift $\Delta E = hc\Delta\bar{\nu} = -\Delta\mu\cdot\Delta F_{matrix}$ depends *both* on the magnitude *and* direction of $\Delta\mu$ and ΔF_{matrix}. Thus, to extract quantitative information on ΔF_{matrix} from observed frequency shifts and understand the correlation between the dispersion in $\bar{\nu}_{CO}$ and $\bar{\nu}_{NO}$ bound to the same set of proteins, it is necessary to consider four factors: the local field correction factor f, the internal angle ζ between $\Delta\mu$ and the transition dipole moment, the absolute direction of the transition dipole moment in the molecular axis system, and the apparent absence of IR-detectable substates for NO bound to Mb.

Uncertainty in the value of the local field correction factor, f, propagates into uncertainty in the value of ΔF_{matrix}. In our analysis of VSE for CO,[4] we presented evidence suggesting that variations in f are small and that the value of f is not much different from 1 for the heme pocket of Mb. This result is supported by recent electrostatics calculations.[32] In the context of comparing results for NO and CO in the same series of proteins, it seems unlikely that the local field correction factor is different when CO vs NO is bound in the heme pocket of Mb, and thus f cancels when taking the ratio $\Delta\mu_{NO}/\Delta\mu_{CO}$.

To determine the absolute direction of $\Delta\mu$, the internal angle ζ between $\Delta\mu$ and the transition dipole moment direction and the direction of the transition dipole moment relative to the molecular axes must be known. For CO bound to heme proteins or to heme in a picket fence model compound, it was possible to measure the VSE as a function of χ, and we obtained $\zeta = 0°$. As shown in Figure 5, $\zeta = 0°$ for NO bound to the picket fence model compound, but it was not possible to obtain this angle for NO bound to the protein because the signal-to-noise ratio becomes much worse when a polarizer is inserted for the polarization measurement. To date, ζ has been found to be 0° for all molecular vibrations,[21,33] and it is difficult to imagine a situation where this would not be the case. Therefore, we assumed that $\zeta = 0°$ for NO bound to the heme iron in the proteins and used this in the calculation of $|\Delta\mu_{NO}|$ using eq 2.

The third issue concerns the absolute direction of the transition dipole moment for the NO oscillator. There has been a huge effort and considerable controversy on this direction for CO bound to heme proteins. Direct measurements by IR spectroscopy on single Mb crystals[8,9] and visible−IR transient dichroism measurements[7] are consistent with the CO transition moment nearly perpendicular to the heme plane. Furthermore, high-resolution X-ray structures show that the CO itself is nearly perpendicular to the heme plane.[34] We are unaware of single-crystal IR or photolysis dichroism data for NO bound to heme. X-ray crystal structures and XAFS data of NO bound to heme in simple model compounds and also NO bound to heme proteins (including Mb) show that NO is bent with respect to the heme plane in the ferrous form while it is almost perpendicular in the ferric form.[35,36] There has been some debate on the degree to which NO is bent in the ferrous form: the

(30) Williams, M. L. Ph.D. Thesis, Bristol University, 1971.
(31) The origin of the $|\Delta\mu|$ will be discussed in a separate communication.
(32) Höfinger, S.; Simonson, T. *Biophys. J.* **2000**. Manuscript submitted.
(33) Chattopadhyay, A.; Boxer, S. G. *J. Am. Chem. Soc.* **1995**, *117*, 1449−1450.
(34) Kachalova, G. S.; Popov, A. N.; Bartunik, H. D. *Science* **1999**, *284*, 473−476.
(35) Brucker, E. A.; Olson, J. S.; IkedaSaito, M.; Phillips, G. N. *Proteins-Structure Function and Genetics* **1998**, *30*, 352−356.
(36) Rich, A. M.; Armstrong, R. S.; Ellis, P. J.; Lay, P. A. *J. Am. Chem. Soc.* **1998**, *120*, 10827−10836.

experimental data for the Fe−N−O angle are scattered in the broad range of 110−155°.

Estimates of the direction of F_{matrix} by electrostatics calculations suggest that its direction varies considerably in different mutants.[10,39] However, the direction and the magnitude of F_{matrix} should be the same for each mutant whether CO or NO is bound *if* they are bound to the same substate, by which we mean a species that has a sufficiently similar average conformation and protonation state reflected in a resolved IR transition. All observed IR spectra of MbNO described here show only a single band (except when there is a Fermi resonance), while there are multiple peaks for the CO bound to V68N, V68D, and V68E.[15] Multiple peaks observed in MbCO spectra are believed to originate, in part, from multiple protonation states of nearby residues.[37] It is quite possible that the signal-to-noise ratio is not good enough to detect lower-intensity subbands for NO in MbNO. The V68E-NO data implies that V68E-NO has multiple substates and that different substates are detected in the photolysis and isotope difference spectra. In making comparisons of data from CO and NO complexes, we will assume that the major peaks in the MbCO and MbNO spectra are from the same substate. It is not unreasonable to assume that they are the same substate and have the same F_{matrix} since the protonation states of most amino acids would not be expected to change whether CO or NO is bound.[38]

Comparisons of $\bar{\nu}_{NO}$ and $\bar{\nu}_{CO}$ in Mb Mutants. With these caveats in mind, the correlation between $\bar{\nu}_{NO}$ and $\bar{\nu}_{CO}$ in Mb variants is shown in Figure 9. The solid dots are from the data in Table 1; the open circles are for other mutants reported in the literature.[10] A reasonably linear relationship is observed between $\bar{\nu}_{CO}$ and $\bar{\nu}_{NO}$, and the best fit to the data obtained in our lab under identical conditions is also shown. The slope of the correlation is 1.0 with an estimated error of 0.2 ($R^2 = 0.90$). Electrostatics calculations of Mb mutants suggest that both the magnitude *and* direction of F_{matrix} vary considerably in the series of distal pocket mutants.[39] The variations in IR peak positions in different mutants, interpreted here as electrochromic band shifts, are due to the different projections of ΔF_{matrix} on $\Delta\mu$. Thus, to the extent that the electrostatics calculations accurately reflect the direction of the matrix electric field, the simplest way to explain the observed correlation is that $\Delta\mu$ for NO has the same projection onto the heme plane as CO bound to Mb. Then, if $\Delta\mu$ for NO bound to Mb is parallel to the transition moment (i.e., $\zeta = 0°$, as found for NO bound to the picket fence porphyrin and for CO bound to Mb)[4] and if the transition moment is parallel to the molecular axis, as for CO bound to Mb,[7,34] we are led to the suggestion that NO and CO have comparable physical orientations. Considering the scatter in the correlation in Figure 9 and the uncertainty in the projection of the diatomic onto the heme plane, this structural conclusion is far from certain, but it does suggest that the Fe(II)−NO bond is not as bent as suggested by some measurements.

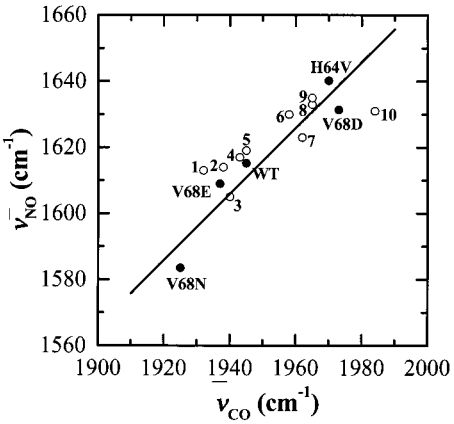

Figure 9. Plot of $\bar{\nu}_{NO}$ versus $\bar{\nu}_{CO}$ for Mb variants. The solid circles are from the isotope difference data reported in this paper; the open circles are taken from ref 10 and correspond to SW Mb (1) L29W ($\bar{\nu}_{NO} = 1613$, $\bar{\nu}_{CO} = 1932$); (2) H64QL29F ($\bar{\nu}_{NO} = 1614$, $\bar{\nu}_{CO} = 1938$); (3) V68F ($\bar{\nu}_{NO} = 1605$, $\bar{\nu}_{CO} = 1940$); (4) V68A ($\bar{\nu}_{NO} = 1617$, $\bar{\nu}_{CO} = 1943$); (5) H64Q ($\bar{\nu}_{NO} = 1619$, $\bar{\nu}_{CO} = 1945$); (6) V68T ($\bar{\nu}_{NO} = 1630$, $\bar{\nu}_{CO} = 1958$); (7) F46V ($\bar{\nu}_{NO} = 1623$, $\bar{\nu}_{CO} = 1962$); (8) H64G ($\bar{\nu}_{NO} = 1633$, $\bar{\nu}_{CO} = 1965$); (9) H64L ($\bar{\nu}_{NO} = 1635$, $\bar{\nu}_{CO} = 1965$); (10) H64VV68T ($\bar{\nu}_{NO} = 1631$, $\bar{\nu}_{CO} = 1984$). The solid line is the best linear fit of solid circles and has a slope of unity.

The slope of the correlation gives the ratio of $\Delta\mu_{CO}/\Delta\mu_{NO}$. The observation that the slope is approximately unity is explained by the observation that the Stark tuning rate for NO and for CO bound to the heme iron are very similar in all mutants. Finally, from the sign of the slope, we can also establish the absolute direction of $\Delta\mu_{NO}$. If $\Delta\mu_{NO}$ points in the same direction as $\Delta\mu_{CO}$, then the NO band shifts should be in the same direction as the CO band shifts, and this is observed. Thus, it can be concluded that $\Delta\mu_{NO}$ points from the oxygen atom to the nitrogen atom as $\Delta\mu_{CO}$ points from the oxygen atom to the carbon atom when CO is bound to heme.[4]

Finally, we can use $\bar{\nu}_{NO}$ of NO bound to heme as a sensitive probe of the changes in the electric field near the heme pocket in Mb. For example, the mutation of His64 to Val, which causes the largest shift (25 cm^{-1}) of $\bar{\nu}_{NO}$ relative to that of WT, changes the electric field by 12.5·f MV/cm pointing from the N atom toward the O atom. Any electrostatic changes in the heme proteins that lead to a spectral shift of $\bar{\nu}_{NO}$ can be treated this way and compared directly with electrostatics calculations.

Acknowledgment. These experiments would not have been possible without the experimental and conceptual contributions by Steven Andrews, and we gratefully acknowledge his many contributions. This work was supported in part by grants from the NSF Chemistry Division and the NIH. The FTIR spectrometer used for these experiments is part of the Stanford Free Electron Laser Center supported by the Office of Naval Research under Contract N00014-94-1-1024.

JA0014741

(37) Muller, J. D.; McMahon, B. H.; Chien, E. Y. T.; Sligar, S. G.; Nienhaus, G. U. *Biophys. J.* **1999**, *77*, 1036−1051.

(38) The pK_a of the amino acids near the heme might be affected by a ligand. At low pH, it is observed that a new CO band appears at 1960 cm^{-1} for WT MbCO, and it is believed that this is an electrochromic band shift due to the protonation of His64 (See refs 4 and 37). Since $\Delta\mu$ of NO is similar to that for CO, it is expected that the same phenomenon should be observed for NO. However, in the range of pH 5.5−7.0, the NO bound to WT Mb has a single band, and the peak position of NO does not change as observed in both photolysis and isotope difference spectra (data not shown).

(39) Electrostatics calculations were done for the distal pocket mutants shown in Figure 9 as open dots and SW wild-type, V68N, V68L, V68I, and H64T (see ref 10). Although the calculation has not been done for the mutants used in the fit, it is expected that they have the same degree of variation in F_{matrix} as the other mutants for which the calculation was done.

(40) There is no obvious way to identify which CO band is from the same substate as the NO band when there are multiple bands for CO bound to Mb. Therefore, the major peak position was used in the comparison with the NO stretch frequency (see the text).